# IMPACT OF THE FORM OF A TRAILER ON ITS AERODYNAMIC PERFORMANCE

Yasar Kocaefe[1]*, Duygu Kocaefe[1], Bruno Gauthier[2]
*Author for correspondence
E-mail: Yasar_Kocaefe@uqac.ca

[1]Department of Applied Sciences, University of Québec at Chicoutimi, 555, boul. de l'Université, Chicoutimi, Québec, Canada
[2]Cycles Devinci, 1555, Rue de la Manic, Chicoutimi, Québec, Canada G7K 1G8

## ABSTRACT

Today, energy efficiency is a topic of great importance not only due to limited energy resources, but also their impact on environment. In the case of vehicles, great effort is being spent on reducing weight and making the form more and more aerodynamic to reduce fuel consumption and increase energy efficiency. However, there is a limit to this form because a vehicle should never lose traction. A highly aerodynamic form reduces the downward force which provides the vehicle its traction.

A trailer with a highly aerodynamic form was investigated to determine if it would lose traction at different speeds and under different wind conditions. Simulations were carried out using the CFD commercial code ANSYS CFX to determine the flow field and the forces (lift, drag, downward force, etc.) around the trailer. The calculation domain was taken large enough not to affect the flow field. The partial differential turbulent flow equations (continuity, momentum, and turbulence equations) were solved in three dimensions to find the velocity and pressure distributions. Different trailer forms were also investigated. The type of vehicle towing the trailer also has an impact on the flow field around it. Thus, different types of vehicles were considered in the simulations. The results demonstrated that certain forms could cause the loss of traction at high enough speeds. In this article, the model is explained, and the results of a number of cases are presented and discussed.

## NOMENCLATURE

***Symbols:***

| | |
|---|---|
| $A$ | area ($m^2$) |
| $C_\mu$ | k- ε turbulence model constant |
| $F$ | force (N) |
| $k$ | turbulence kinetic energy ($m^2\ s^{-2}$) |
| $P$ | pressure (Pa) |
| $P_k$ | shear production of turbulent kinetic energy ($m^2\ s^{-3}$) |
| $S_m$ | source term for momentum equation ($kg\ m^{-2}\ s^{-2}$) |
| $t$ | time (s) |
| $U$ | velocity ($m\ s^{-1}$) |

***Greek letters***

| | |
|---|---|
| $\rho$ | density ($kg\ m^{-3}$) |
| $\mu$ | viscosity ($kg\ m^{-1}\ s^{-1}$) |
| $\varepsilon$ | turbulence eddy dissipation ($m^2\ s^{-3}$) |
| $\sigma_{k\ or\ \varepsilon}$ | turbulent Prandtl numbers of k or ε |
| $\tau$ | shear stress ($N\ m^{-2}$) |

***Subscripts:***

| | |
|---|---|
| $D$ | drag |
| $eff$ | effective |
| $L$ | lift |
| $n$ | normal |
| $p$ | parallel |
| $t$ | turbulent |
| $V$ | vertical (downward) |
| $W$ | weight |

## INTRODUCTION

Transportation is one of the major sources of greenhouse gas emissions and acid rain due to the presence of gases such as $CO_2$, CO, $NO_x$, $SO_2$ and particles in the exhaust [1-2]. Also, limited resources require the efficient use of available fuel. Over the past few decades, a great deal of effort has been spent to increase the energy efficiency in the field of transportation (cars, trains, airplanes, boats, etc.) [3-4]. In the case of cars, two major developments are the use of aerodynamic body forms to reduce drag (resistance) force and lighter materials to decrease the weight of vehicles [4-5].

The drag coefficient has been reduced by almost threefold over the past 100 years (approximately from 0.60 to 0.25) [5]. This is still far from the theoretical limit (about 0.12-0.15) [5]; however, further changes should not compromise the safety and the utility of the vehicle. An aerodynamic form could be susceptible to the loss of traction of the vehicle at high speeds.

In the case of trailers, the flow field around the vehicle, especially the flow structure in the wake region, influences the flow around the trailer. Thus, the combination of vehicle and trailer has to be investigated together to determine accurately the forces acting around the trailer.

The forces acting on a body in a flow field consist of pressure forces perpendicular to the surface and shear forces (also called shear stress) parallel to the surface of that body. These forces create a resultant force in the three dimensional space. In the case of symmetrical bodies such as cars, planes, and trains, the lateral component becomes zero if the flow is parallel to the symmetry plane. Of the remaining two components, the one that acts parallel to the free-stream direction is called the drag force and the other that acts normal to the free-stream direction is called the lift force. For airplanes, the lift force should exceed the weight of the plane. Contrarily, for cars, there should always be traction (adherence to the road), and the downward force should always be greater than zero [4-5].

In this project, a number of trailer geometries were studied to determine the possible loss of traction at high enough speeds. Since the vehicle towing the trailer has an impact on the flow calculations around the trailer, two types of vehicles were considered, a sedan and a sports utility vehicle (SUV). The drag, lift, and downward forces were calculated. In a few cases, the impact of cross-wind was also investigated.

## SYSTEM

The system consisted of a trailer towed by a vehicle. Three different trailer geometries were examined:

- streamlined,
- box-shaped, and
- streamlined with a nose.

These are shown in Figure 1. For the vehicle, two different cases were considered: a sedan and an SUV. Figure 2 shows the two vehicles with the trailer which has a 'streamlined with nose' geometry. Different vehicle and trailer combinations were simulated. The simulations were carried out using the commercial CFD code ANSYS CFX [6].

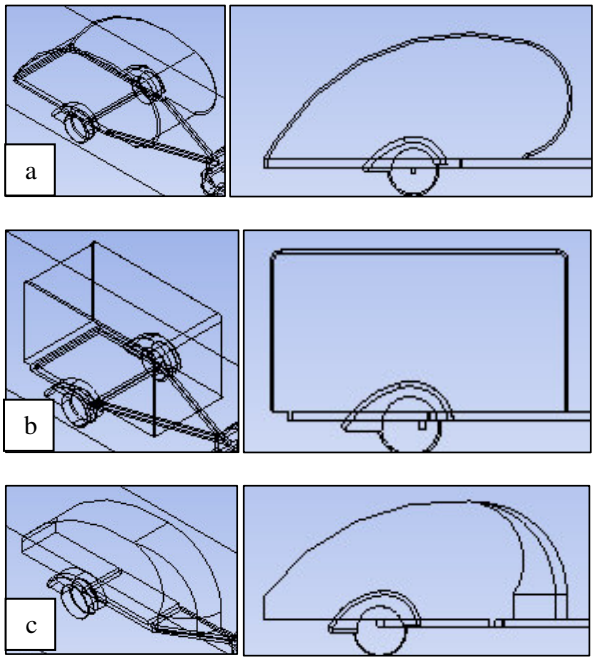


Figure 1: Trailer Geometries Considered: (a) Streamlined, (b) Box-shaped, (c) Streamlined with Nose

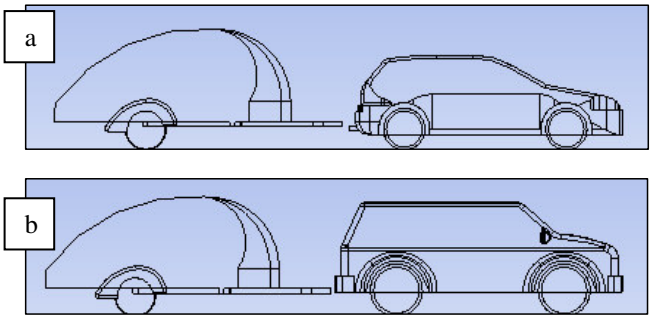


Figure 2: Vehicles Considered with the 'Streamlined with Nose' Trailer: (a) a Sedan, (b) an SUV

## MATHEMATICAL MODEL

A large flow domain was taken to ensure that the flow calculated around the trailer is independent of the domain size and the forces are determined accurately. Examples for two flow domains used in this work are given in Figure 3. For the cases with cross-wind, the complete geometry of the trailer and the vehicle was taken to calculate the lateral force as well (Figure 3 a). For the cases without wind, half of the trailer and half of the vehicle were considered (Figure 3 b).

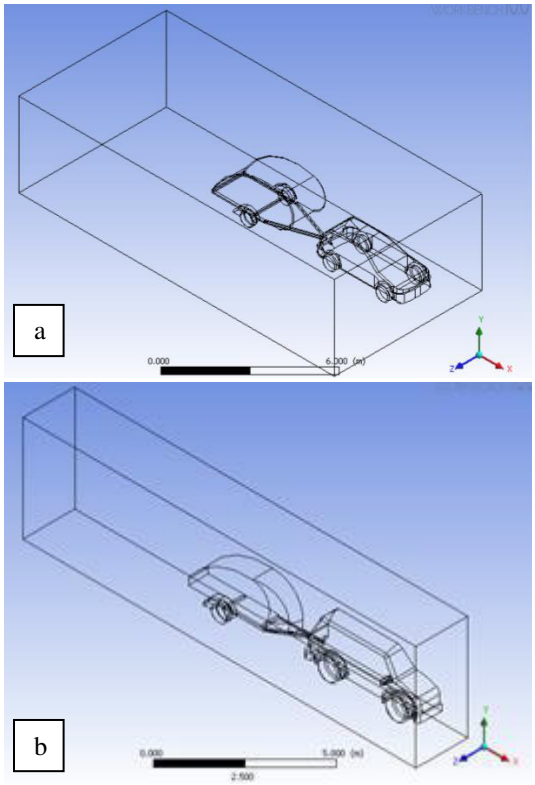


Figure 3: Flow Domains for the Simulations: (a) Sedan and 'Streamlined' Trailer for Cross-Wind Cases, (b) SUV and 'Streamlined with Nose' Trailer for Cases Without Wind

When there is no wind (see, for example, Figure 3 b), the freestream flow is parallel to the symmetry plane of the system. Thus, only half geometry is necessary. The vehicle and the trailer were taken as stationary; the air velocity was assigned the speed (60, 100, 140 km/h) being simulated at the inlet since the relative velocity is the key for the calculation of forces. The bottom surface was considered as a non-slip wall. Apart from the symmetry plane, other lateral surfaces were assigned free-slip condition.

With cross winds, the entire geometry needs to be taken into account. Thus, a larger flow domain was used in the simulations (see, for example, Figure 3 a). The components of the cross-wind (depending on the direction) were added to those of the air velocity (vehicle speed). In this case, only the top surface was assigned a free-slip condition; and there was no symmetry plane.

### 1. Calculation of flow field

In order to solve for turbulent flow around the vehicle and the trailer, the following equations were considered [6]. The

continuity equation ensures the mass balance:

$$\frac{\partial \rho}{\partial t} + \nabla \cdot (\rho U) = 0 \tag{1}$$

where $\rho$ is the density and $U$ is the air velocity.

The instantaneous momentum equation (Navier-Stokes) is written as:

$$\frac{\partial (\rho U)}{\partial t} + \nabla \cdot (\rho U \otimes U) = -\nabla P + \nabla \cdot \tau + S_M \tag{2}$$

where $S_M$ is the source term and $\tau$ is the shear stress tensor given by:

$$\tau = \mu \left( \nabla U + (\nabla U)^T - \frac{2}{3} \delta \nabla \cdot U \right) \tag{3}$$

The turbulence was represented by the $k - \varepsilon$ model (k: turbulence kinetic energy; ε: turbulence eddy dissipation). This model gives fairly good results with reasonable numerical effort in a large number of fluid flow cases. In this approach, the variables are averaged based on the assumption that the Reynolds stresses are related to the mean velocity gradients through the turbulent viscosity. With the introduction of these two variables, the momentum equation becomes:

$$\begin{aligned} &\frac{\partial (\rho U)}{\partial t} + \nabla \cdot (\rho U \otimes U) = -\nabla P' + \\ &\nabla \cdot \left( \mu_{eff} \left( \nabla U + (\nabla U)^T - \frac{2}{3} \delta \nabla \cdot U \right) \right) + S_M \end{aligned} \tag{4}$$

where $P'$ is the modified pressure given by:

$$P' = P + \frac{2}{3} \rho k + \frac{2}{3} \mu_{eff} \nabla \cdot U \tag{5}$$

with $\mu_{eff}$, effective viscosity, is the sum of dynamic viscosity $\mu$ and turbulent viscosity $\mu_t$ :

$$\mu_{eff} = \mu + \mu_t \tag{6}$$

The turbulent viscosity is defined by:

$$\mu_t = C_\mu \rho \frac{k^2}{\varepsilon} \tag{7}$$

where $C_\mu$ is a constant.

The term $\vec{\nabla} . (\rho \vec{U} \otimes \vec{U})$ represents:

$$\begin{aligned} &\vec{\nabla} . (\rho \vec{U} \otimes \vec{U}) \\ &= \begin{pmatrix} \frac{\partial}{\partial x}(\rho U_x U_x) + \frac{\partial}{\partial y}(\rho U_y U_x) + \frac{\partial}{\partial z}(\rho U_z U_x) \\ \frac{\partial}{\partial x}(\rho U_x U_y) + \frac{\partial}{\partial y}(\rho U_y U_y) + \frac{\partial}{\partial z}(\rho U_z U_y) \\ \frac{\partial}{\partial x}(\rho U_x U_z) + \frac{\partial}{\partial y}(\rho U_y U_z) + \frac{\partial}{\partial z}(\rho U_z U_z) \end{pmatrix} \end{aligned} \tag{8}$$

The values of $k$ and $\varepsilon$ are obtained from the solution of the following partial differential equations:

$$\begin{aligned} &\frac{\partial (\rho k)}{\partial t} + \nabla \cdot (\rho\, U\, k) \\ &= \nabla \cdot \left[ \left( \mu + \frac{\mu_t}{\sigma_k} \right) \nabla k \right] + P_k - \rho\, \varepsilon \end{aligned} \tag{9}$$

$$\begin{aligned} &\frac{\partial (\rho \varepsilon)}{\partial t} + \nabla \cdot (\rho\, U\, \varepsilon) \\ &= \nabla \cdot \left[ \left( \mu + \frac{\mu_t}{\sigma_\varepsilon} \right) \nabla \varepsilon \right] + \frac{\varepsilon}{k} (C_{\varepsilon 1}\, P_k - C_{\varepsilon 2} \rho\, \varepsilon) \end{aligned} \tag{10}$$

where $C_{\varepsilon 1}$, $C_{\varepsilon 2}$, $C_\mu$ are the constants of the $k - \varepsilon$ model.

### 2. Determination of body forces

After the calculation of detailed pressure and velocity distributions around the trailer, the shear stress distribution on the surface was found [4-5]. Then, the lift ($F_L$) and drag ($F_D$) forces were determined from:

$$F_L = \int (P_n + \tau_n)\, dA \tag{11}$$

$$F_D = \int (P_p + \tau_p)\, dA \tag{12}$$

where n and p denote normal and parallel components to the free-stream direction of pressure and shear forces.

A vehicle should never lose traction (contact with the road surface). This is ensured if the net vertical force ($F_V$) acting on the car is downwards. This can be calculated from:

$$F_V = F_W - F_L \tag{13}$$

where $F_W$ is the weight of the vehicle. The vehicle losses traction when $F_V \leq 0$. The drag force is a resistance, and the sum of the drag force with the friction due to traction gives the total resistance that is responsible for fuel consumption.

### 3. Numerical Parameters and Mesh

The domain was divided into 220,292 nodes for the cases without wind (see Figure 3 b). A non-uniform mesh was used with small nodes around the vehicles and the trailers. The convergence criterion was the reduction of residuals to less than $10^{-5}$. On a PC with an Intel(R) Xeon(R) 3.10 GHz processor and 16 Go RAM, the computation time was 36 min. For the domain used in cross-wind simulations (see Figure 3 a), the number of nodes was tripled, which also increased the computation time by about three times. The mesh is shown in Figure 4 for the 'no wind' domain given in Figure 3 b.

## RESULTS AND DISCUSSION

### 1. Simulation Results

Simulations were carried out for various cases, and the velocity and pressure distributions were obtained. Figure 5 presents (a) the velocity and (b) pressure fields on a plane close to the symmetry plane for the case shown in Figures 2 b and 3b at 100 km/h. The stagnation zone in front of the SUV and the recirculation zones behind the SUV and the trailer can be seen. The forces were calculated based on these distributions, which are discussed in the following sections.

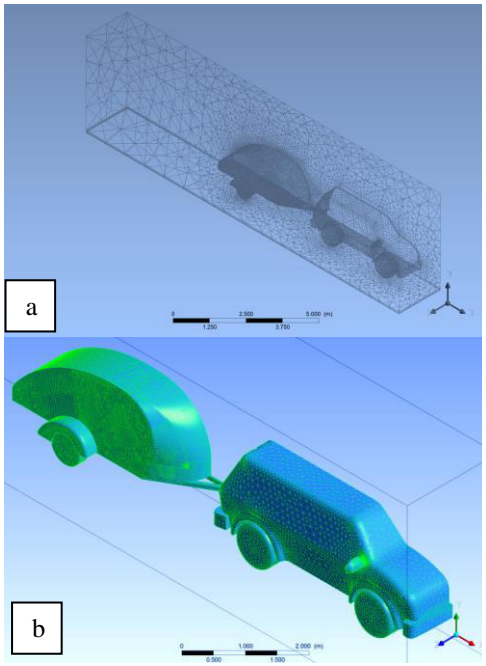


Figure 4: (a) Non-uniform Mesh for the Whole Domain; (b) Fine Mesh on the Surface of the Trailer and SUV (No Wind)

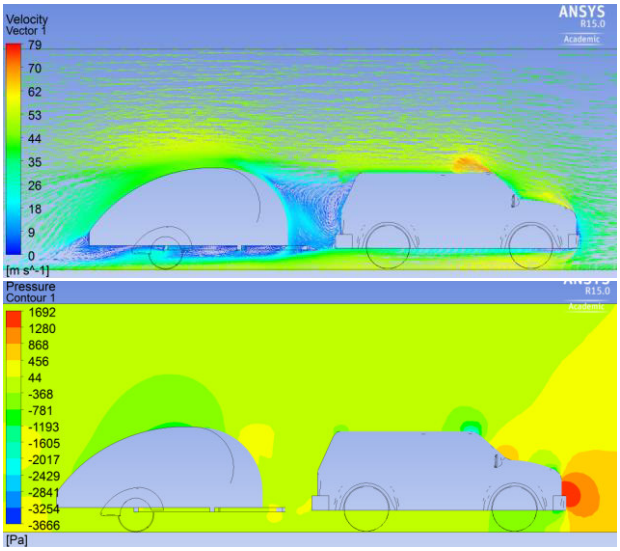


Figure 5: SUV with the 'Streamlined with Nose' Trailer at 100 km/h and Without Wind: (a) Velocity and (b) Pressure Fields

## 2. Effect of Trailer Geometry (with Sedan)

The effect of the trailer geometry on drag, lift, and downward forces are shown in Figures 6, 7, and 8, respectively, for the vehicle (a sedan) and the trailer. Figure 6 a shows that there is some effect, but the drag force is generally similar for the vehicle for all trailer geometries. For the trailers (Figure 6 b), the geometry has a significant impact. Box-shaped geometry gives the greatest drag force as expected. The addition of a nose to the streamlined geometry increases the drag as well. Also, the drag force for the vehicle is much lower than that for the trailers. It is also interesting to note that the drag force is small for speeds less than 60 km/h; then, it increases drastically due to its dependence on the square of the velocity.

Figure 7 a indicates that the lift force for the vehicle is also similar for different trailer geometries. The lift force for the box-shaped trailer is the smallest as expected (Figure 7 b). Streamlined trailer geometry gives higher lift force; and the addition of a nose seems to increase the lift force even more (Figure 7 b). Again, the lift force for the trailer is much greater than that for the vehicle.

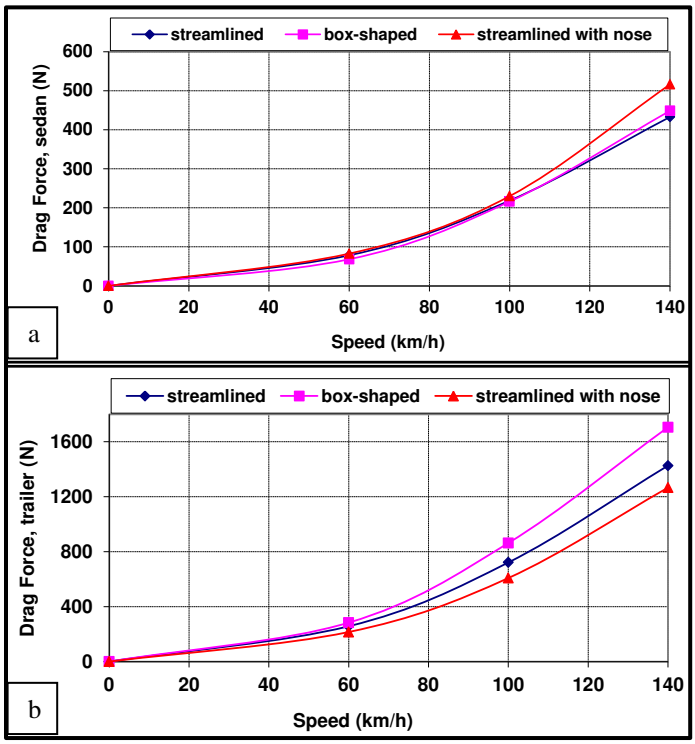


Figure 6: Drag Force for (a) the Vehicle and (b) the Trailer for Different Trailer Geometries

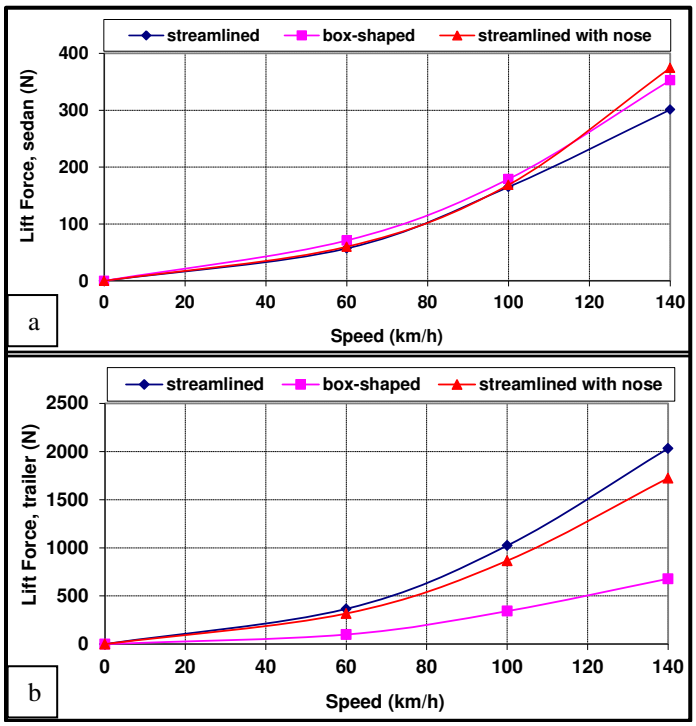


Figure 7: Lift Force for (a) the Vehicle and (b) the Trailer for Different Trailer Geometries

The downward forces (the net force in the downward direction) are presented in Figure 8. For the vehicle, the downward force differs little with the trailer geometry. For the trailer, however, this force varies significantly depending on the trailer shape. The box-shaped trailer has the greatest value as expected. The streamlined shape reduces the downward force drastically, resulting in even negative values (lift) above 130 km/h. The addition of a nose seems to increase the value somewhat, but still the force is nearly zero at speeds close to 140 km/h. These results indicate clearly that highly aerodynamic trailer forms could result in the loss of traction. Thus, design should include features to ensure traction.

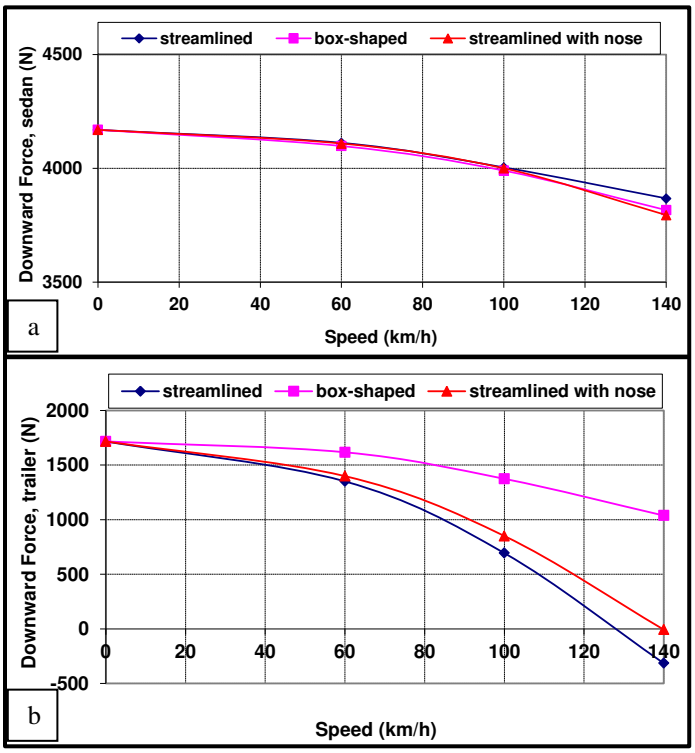


Figure 8: Downward Force for (a) the Vehicle and (b) the Trailer for Different Trailer Geometries

### 3. Effect of Vehicle Type (with 'Streamlined with Nose' Trailer Geometry)

The effect of the vehicle type on the forces around the trailer (with 'streamlined with nose' geometry) was studied for a sedan and an SUV. The results are given in Figures 9, 10, and 11 for the drag, lift, and downward forces, respectively.

Figure 9 presents the drag forces calculated for both the vehicle and the trailer. As expected, SUV has much higher drag (Figure 9 a). The trailer on the other hand shows the reverse trend: the trailer behind an SUV has a lower drag force compared to the one towed by a sedan (Figure 9 b). The flow field (the wake) behind the SUV seems to have a significant impact on the flow field around the trailer, reducing the drag.

Figure 10 shows the lift forces calculated for both the vehicle and the trailer. SUV has much lower lift (Figure 10 a) as expected. The lift force for the trailer does not seem to vary much (Figure 10 b); but, the trailer behind a sedan has a higher lift force compared to the one towed by an SUV. The flow field (the wake) behind the SUV lowers the lift as well.

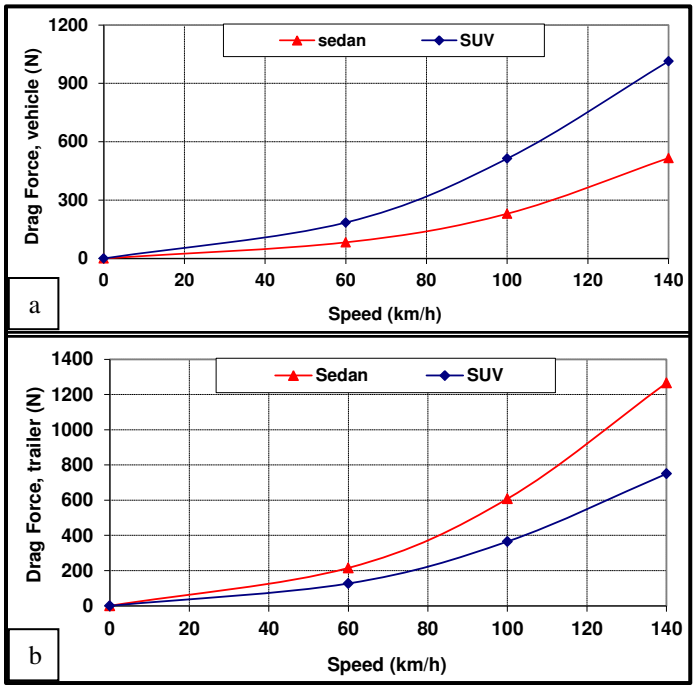


Figure 9: Drag Force for (a) the Vehicle and (b) the Trailer for Different Types of Vehicles

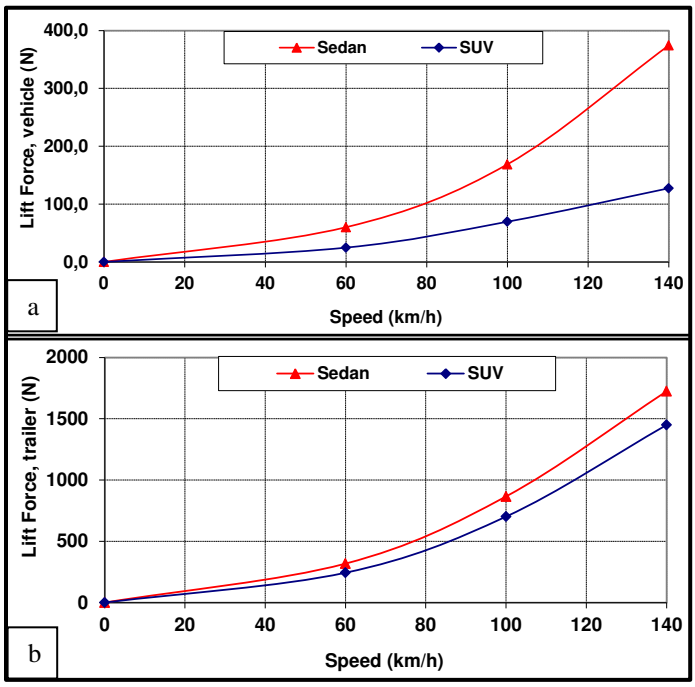


Figure 10: Lift Force for (a) the Vehicle and (b) the Trailer for Different Types of Vehicles

The downward forces are given in Figure 11. They are both high, and there is no risk of traction loss for the vehicles as indicated by Figure 11 a. As expected, the downward forces decrease slightly as a function of speed due to increase in lift. Also, the force for SUV is almost twice as much as the one for sedan mainly because of the greater weight of SUV. For the trailer (Figure 11 b), the downward force approaches zero with increasing speed above 120 km/h. As shown above, the trailer towed by an SUV has lower lift compared to the one with a

sedan; as a results, the downward force is greater for the trailer pulled by an SUV. The trailer behind a sedan on the other hand has zero traction at 140 km/h (the downward force is slightly negative). The results indicate that there is a risk of losing traction for the trailer at high speeds especially if pulled by a sedan.

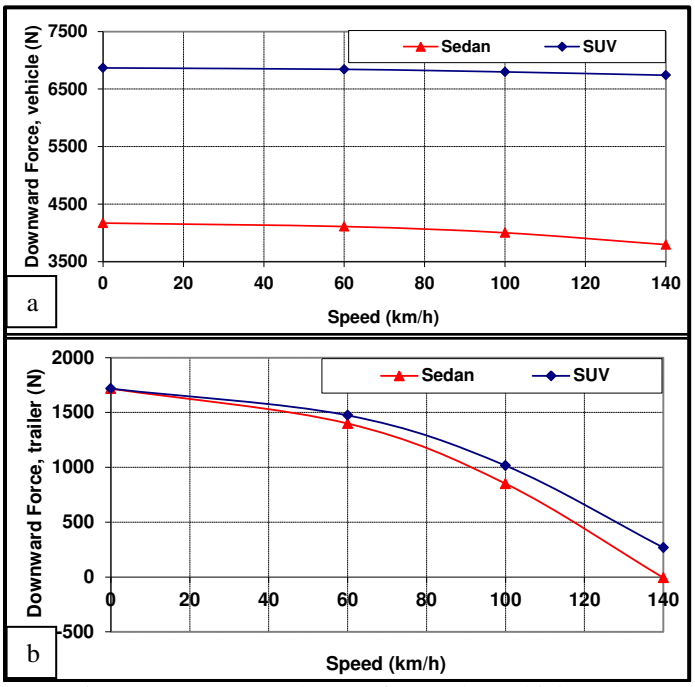


Figure 11: Downward Force for (a) the Vehicle and (b) the Trailer for Different Types of Vehicles

### 4. Effect of Cross-Wind

The effect of a cross-wind was also studied for a few cases. Results are shown in Table 1 for a head wind of 35 km/h at 45° (angle between the direction of travel and the wind) for a sedan pulling a trailer of 'streamlined' or 'box-shaped' geometry at 100 and 140 km/h.

As observed before, the drag and lift forces increase and the downward force decreases with speed. The downward force becomes negative for the streamlined trailer at 140 km/h indicating the loss of traction at such high speeds. In all the previous cases, the lateral force was zero since the flow was due to the vehicle motion which is parallel to the symmetry plane. Here, as Table 1 indicates, there are significant lateral (side) forces, and they increase drastically as the speed goes up from 100 to 140 km/h. Thus, decreasing downward forces accompanied by strong lateral forces could even overturn the trailer in the case of highly aerodynamic cases.

## CONCLUSIONS

Simulations were carried out to determine the impact of the trailer geometry and the effect of the type of vehicle pulling the trailer on the acting body forces around both the trailer and the vehicle. Also, the risk of traction loss was evaluated at different speeds. The results indicate clearly that a highly aerodynamic trailer shape could reduce the downward force to low values (even to zero) which would result in the loss of traction.

The results also show that the flow field around the trailer is affected significantly by the type of vehicle pulling it. This alters the forces acting on the body and may reduce or increase the risk of traction loss. In addition, cross-winds, depending on its speed, could also generate strong lateral forces which may overturn the trailer.

Table 1: Forces Acting on the Vehicle and the Trailer Under Cross-Wind Conditions

| Speed (km/h) | | Drag Force (N) | Lift Force (N) | Downward Force (N) | Lateral Force (N) |
|---|---|---|---|---|---|
| | | **With Streamlined Trailer** | | | |
| **100** | sedan | 2297 | 2270 | 6068 | 3628 |
| | trailer | 1814 | 2315 | 1119 | 3486 |
| **140** | sedan | 3501 | 3154 | 5185 | 5078 |
| | trailer | 3508 | 4070 | ***(636)**** | 6070 |
| | | **With Box-Shaped Trailer** | | | |
| **100** | sedan | 2138 | 2336 | 6003 | 3687 |
| | trailer | 2450 | 1763 | 1670 | 3686 |
| **140** | sedan | 3092 | 3380 | 4959 | 5013 |
| | trailer | 5304 | 2588 | 845 | 5678 |

*The value in parenthesis is negative.

## REFERENCES


1. F.M. Vanek, L. Albright, L. Angenent, *Energy Systems Engineering: Evaluation and Implementation*, 2nd Edition, McGraw Hill, N.Y., 2012.
2. Statistics Canada, "Report on Energy Supply and Demand in Canada, 2013", Minister of Industry, February 2015.
3. J.D. Anderson Jr., *Fundamentals of Aerodynamics*, 5th Edition, McGraw Hill, N.Y., 2010.
4. F.M. White, *Fluid Mechanics*, 7th Edition, McGraw Hill, New York, N.Y., 2011.
5. *Aerodynamics of road vehicles: from fluid mechanics to vehicle engineering*, 4th Edition, Ed.: W.H. Hucho, Society of Automotive Engineers, Warrendale, Pa., 1998.
6. *ANSYS CFX-Solver Theory Guide*, ANSYS Inc., Canonsburg, PA., 2013.